Hydrothermal Synthesis and Structural Characterization of a Series of One-Dimensional Organic/Inorganic Hybrid Materials of the $[(MoO_3)_n(2,2'\text{-bipy})_m]$ Family: $[MoO_3(2,2'\text{-bipy})]$, $[Mo_2O_6(2,2'\text{-bipy})]$, and $[Mo_3O_9(2,2'\text{-bipy})_2]$

Pamela J. Zapf,[†] Robert C. Haushalter,[‡] and Jon Zubieta*,[†]

Department of Chemistry, Syracuse University, Syracuse, New York 13244, and NEC Research Institute, 4 Independence Way, Princeton, New Jersey 08540

Received April 29, 1997. Revised Manuscript Received July 10, 1997[⊗]

Three one-dimensional molybdenum oxide/2,2′-bipyridine species have been prepared by hydrothermal methods and structurally characterized. The reaction of MoO_3, 2,2′-bipyridine, and H_2O in the mole ratio 1:0.68:680 at 160 °C for 120 h in a 23 mL Teflon-lined Parr acid digestion bomb produces colorless rods of $[MoO_3(2,2'\text{-bipy})]$ (**1**) mixed with colorless octahedra of $[Mo_3O_9(2,2'\text{-bipy})_2]$ (**3**). The structure of **1** consists of one-dimensional chains of corner-sharing distorted $\{MoO_4N_2\}$ octahedra. $[Mo_2O_6(2,2'\text{-bipy})]$ (**2**) was prepared from a mixture of $Na_2MoO_4{\cdot}2H_2O$, MoO_3, 2,2′-bipyridine, $MnCl_2{\cdot}4H_2O$, and H_2O in the mole ratio 1:1:2:1.9:263 and was isolated as colorless plates. In contrast to the structure of **1**, compound **2** consists of a chain of alternating corner-sharing $\{MoO_4N_2\}$ octahedra and $\{MoO_4\}$ tetrahedra. Compound **3** was isolated as colorless octahedra. The structure of **3** consists of a chain of corner-sharing $\{MoO_4N_2\}$ octahedra and $\{MoO_4\}$ tetrahedra that alternate such that each $\{MoO_4N_2\}$ octahedron corner-shares with another such octahedron and a $\{MoO_4\}$ tetrahedron; consequently, each $\{MoO_4\}$ unit corner shares with two $\{MoO_4N_2\}$ octahedra. Crystal data: **1**: monoclinic *Cc*, $a = 14.246(3)$, $b = 9.628(2)$, $c = 7.344(1)$ Å, $\beta = 101.26(3)°$, $V = 987.9(3)$ Å^3, $Z = 4$, $D_{calc} = 2.018$ g cm^{-3}; structure solution and refinement based on 1346 reflections converged at $R = 0.026$; **2**: monoclinic $P2_1/m$, $a = 9.0875(6)$, $b = 6.8286(5)$, $c = 10.5441(7)$ Å, $\beta = 99.307(2)°$, $V = 645.70(8)$ Å^3, $Z = 2$, $D_{calc} = 2.284$ g cm^{-3}, structure solution and refinement based on 1607 reflections converged at $R = 0.062$; **3**: monoclinic $P2_1/n$, $a = 13.5468(3)$, $b = 10.1407(2)$, $c = 17.8346(1)$ Å, $\beta = 104.888(1)°$, $V = 2367.76(7)$ Å^3, $Z = 4$, $D_{calc} = 2.088$ g cm^{-3}, structure solution and refinement based on 5581 reflections converged at $R = 0.054$.

Introduction

Considerable attention has been focused on metal oxide based solid phases due to their applications in catalysis, sorption, molecular electronics, energy storage, optical materials, and ceramics.[1,2] The evolution of metal oxide chemistry is dependent upon the synthesis of new solids possessing unique structures and properties,[3] although synthesis of these materials remains a challenge.[4,5] Combining hydrothermal techniques with the structure-directing properties of organic components provides a strategy for the isolation of metastable inorganic/organic composites which retain some structural features of their synthetic precursors.[6] The cooperative assembly of molybdenum oxide/organic phases was first demonstrated with the isolation and characterization of $[H_3NCH_2CH_2NH_3][Mo_3O_{10}]$.[7] An extensive structural chemistry for such composite oxide materials was suggested by the subsequent characterization of the one-dimensional phases $[H_3N(CH_2)_6NH_3][Mo_4O_{13}]$ and $Na(NH_4)[Mo_3O_{10}]$.[8]

Polymeric structures based on infinite one-dimensional chains of oxomolybdenum polyhedra are characteristic of the dimolybdate and trimolybdate systems.[9−14] However, examination of the structures of $[H_3NCH_2CH_2NH_3][Mo_3O_{10}]$,[7] $K_2[Mo_3O_{10}]$,[14] $(NH_4)_2[Mo_3O_{10}]$,[11] and $Na(NH_4)[Mo_3O_{10}]$[8] and of the related tetramolybdate $[H_3N(CH_2)_6NH_3][Mo_4O_{13}]$[8] reveals that although all share a common one-dimensional framework, there are marked differences in their polyhedral connectivities. A common thread in the structural chemistry of these species is the occurrence of edge-sharing between adjacent polyhedra as part of their structural motif. Examination of the title compounds reveals the absence

[†] Syracuse University.
[‡] NEC Research Institute.
[⊗] Abstract published in *Advance ACS Abstracts,* August 15, 1997.

(1) Cheetham, A. J. *Science* **1994**, *264*, 794 and references therein.
(2) Cox, P. A. *Transition Metal Oxides*; Clarendon Press: Oxford, England, 1995.
(3) Bhuvanesh, N. S. P.; Prasad, B. R.; Subramanian, C. K.; Gopalakrishnan, J. *Chem. Commun.* **1996**, 289.
(4) Stein, A.; Keller, S.; Mallouk, T. E. *Science* **1993**, *259*, 1558.
(5) DiSalvo, F. J. *Science* **1990**, *247*, 649.
(6) Gopalakrishnan, J. *Chem. Mater.* **1995**, *7*, 1265.
(7) Khan, M. I.; Chen, Q.; Zubieta, J. *Inorg. Chim. Acta* **1993**, *213*, 325.
(8) Xu, Y.; An, L.-H.; Koh, L.-L. *Chem. Mater.* **1996**, *8*, 814.
(9) Armour, A. W.; Drew, M. G. B.; Mitchell, P. C. H. *J. Chem. Soc., Dalton Trans.* **1975**, 1493.
(10) Seleborg, M. *Acta Chem. Scand.* **1967**, *21*, 499.
(11) Range, K.; Fässler, A. *Acta Crystallogr., Sect. C* **1990**, *46*, 488.
(12) Kreusler, H.-U.; Förster, A.; Fuchs, J. *Z. Naturforsch., B* **1980**, *35*, 242.
(13) Hodorowicz, S. A.; Lasocha, W. *Cryst. Res. Technol.* **1988**, *23*, 3, K43.
(14) Gatehouse, B. M.; Leverett, P. *J. Chem. Soc. A* **1968**, 1398.

S0897-4756(97)00260-3 CCC: $14.00

Table 1. Crystallographic Data for the One-Dimensional Solids [MoO_3(2,2′-bipy)] (1), [Mo_2O_6(2,2′-bipy)] (2), and [Mo_3O_9(2,2′-bipy)$_2$] (3)

	1	2	3
chemical formula	$C_{10}H_8MoN_2O_3$	$C_{10}H_8Mo_2N_2O_6$	$C_{20}H_{16}Mo_3N_4O_9$
a, Å	14.246(3)	9.0875(6)	13.5468(3)
b, Å	9.628(2)	6.8286(5)	10.1407(2)
c, Å	7.3440(10)	10.5441(7)	17.83460(10)
β, deg	101.26(3)	99.307(2)	104.8880(10)
V, Å^3	987.9(3)	645.70(8)	2367.76(7)
Z	4	2	4
formula weight	300.1	444.06	744.19
space group	Cc	$P2_1/m$	$P2_1/n$
T, °C	−20	25	25
λ, Å	0.71063	0.71073	0.71073
D_{calc}, g cm^{-3}	2.018	2.284	2.088
μ, mm^{-1}	1.319	1.968	1.624
R[a]	0.0264	0.0623	0.0541
R_w[b]	0.0282		
wR_2[c]		0.0965	0.0849

[a] $\sum||F_o| - |F_c||/|F_o|$. [b] $[\sum w(|F_o| - |F_c|)^2/\sum w|F_o|^2]^{1/2}$. [c] $[\sum[w(F_o^2 - F_c^2)^2]/\sum[w(F_o^2)^2]]^{1/2}$.

of edge-sharing interactions, an observation that can be attributed to the introduction of the bipyridyl ligand which serves to "passivate" the molybdenum oxide coordination sphere by blocking further Mo−oxo bond formation and apparently limiting the aggregation process to corner-sharing linkages.

While crystal "engineering" based on transition-metal coordination to appropriate ligands has evolved dramatically since the seminal work of Robson and Hoskins,[15,16] applications to metal oxides have remained largely unexplored. Herein, we report the syntheses and structural characterization of a series of inorganic/organic composite materials incorporating 2,2′-bipyridine components as ligands, represented by three members of the new family of materials [$(MoO_3)_n$-(2,2′-bipy)$_m$]: [MoO_3(2,2′-bipy)] (**1**), [Mo_2O_6(2,2′-bipy)] (**2**), and [Mo_3O_9(2,2′-bipy)$_2$] (**3**).

Experimental Section

All chemicals were used as delivered from Aldrich without further purification. The Teflon-lined stainless steel acid digestion bombs were purchased from Parr Instrument Co.

Preparation of [MoO_3(2,2′-bipy)] (1). *Method A*: A mixture of $Na_2MoO_4{\cdot}2H_2O$, MoO_3, 2,2′-bipyridine, $FeCl_2{\cdot}4H_2O$ and H_2O in the mole ratio 1:0.84:1.6:0.82:474 (6 mL volume) was placed in a 23 mL Teflon-lined Parr acid digestion bomb and heated for 48 h at 160 °C under autogenous pressure. The reaction mixture was removed from the oven and allowed to cool at ambient conditions, whereupon colorless rods of **1** were collected by mechanical separation in ca. 10% yield based on molybdenum.

Method B: A mixture of MoO_3, 2,2′-bipyridine, and H_2O in the mole ratio 1:0.68:680 (8 mL volume) was placed in a Parr acid digestion bomb and heated at 160 °C for 120 h under autogenous pressure. The reaction mixture was removed from the oven and allowed to cool under ambient conditions for 3 h. Colorless rods of **1** were collected by mechanical separation from a mixture of **1** and colorless octahedra of **3**.

Preparation of [Mo_2O_6(2,2′-bipy)] (2). A mixture of $Na_2MoO_4{\cdot}2H_2O$, MoO_3, 2,2′-bipyridine, $MnCl_2{\cdot}2H_2O$, and H_2O in the mole ratio 1:1:2:1.9:2630 (8 mL volume) was placed in a 23 mL Teflon-lined Parr acid digestion bomb and heated for 4 d at 200 °C under autogenous pressure. After allowing the reaction mixture to cool for 3 h, colorless plates of **2** were

(15) Robson, R.; Abraham, D. P.; Batten, S. R.; Gable, R. W.; Hoskins, B. F.; Liu, J. *Supramolecular Architecture*; Bein, T., Ed.; *ACS Symposium Series*; **1992**, *499*, 256.
(16) Abraham, D. P.; Hoskins, B. F.; Robson, R. *J. Am. Chem. Soc.* **1991**, *113*, 3603.

Table 2. Atomic Positional Parameters (×10^4) and Equivalent Isotropic Displacement Coefficients (Å^2 × 10^3) for [MoO_3(2,2′-bipy)] (1), [Mo_2O_6(2,2′-bipy)] (2), and [Mo_3O_9(2,2′-bipy)$_2$] (3)

	x	*y*	*z*	*U*(eq)
		1		
Mo	1789	260(1)	11203	15(1)
O(1)	2014(3)	1969(4)	10709(6)	29(1)
O(2)	2894(3)	−559(4)	11704(5)	29(1)
O(3)	1519(3)	393(4)	13522(5)	23(1)
N(1)	139(3)	624(5)	10277(6)	21(1)
N(2)	934(3)	−1842(4)	11132(6)	18(1)
C(1)	−221(4)	1896(7)	9916(8)	28(2)
C(2)	−1195(5)	2163(7)	9398(9)	34(2)
C(3)	−1813(5)	1061(8)	9246(9)	36(2)
C(4)	−1461(4)	−255(8)	9638(8)	32(2)
C(5)	−475(4)	−465(6)	10134(7)	21(2)
C(6)	−27(4)	−1846(6)	10536(7)	21(2)
C(7)	−547(5)	−3069(7)	10347(10)	37(2)
C(8)	−76(6)	−4303(8)	10815(12)	48(3)
C(9)	902(5)	−4301(7)	11412(10)	41(2)
C(10)	1373(4)	−3046(6)	11592(8)	29(2)
		2		
Mo(1)	−8(1)	2500	8142(1)	18(1)
Mo(2)	−1586(1)	−2500	7625(1)	23(1)
O(1)	1434(8)	2500	7298(8)	34(2)
O(2)	762(9)	2500	9730(7)	34(2)
O(3)	−459(5)	−287(7)	7989(5)	32(1)
O(4)	−2085(9)	−2500	6001(8)	43(2)
O(5)	−3236(8)	−2500	8204(8)	36(2)
N(1)	−1716(9)	2500	6255(8)	21(2)
N(2)	−2427(9)	2500	8581(8)	22(2)
C(1)	−1282(13)	2500	5102(10)	39(3)
C(2)	−2285(15)	2500	3958(12)	67(5)
C(3)	−3767(16)	2500	4017(12)	59(4)
C(4)	−4239(13)	2500	5188(11)	38(3)
C(5)	−3179(11)	2500	6301(10)	24(2)
C(6)	−3618(12)	2500	7624(10)	28(2)
C(7)	−5056(11)	2500	7862(11)	33(3)
C(8)	−5321(14)	2500	9106(13)	45(3)
C(9)	−4094(14)	2500	10087(11)	44(3)
C(10)	−2713(14)	2500	9791(12)	42(3)
		3		
Mo(1)	3165(1)	8516(1)	1222(1)	20(1)
Mo(2)	2257(1)	6934(1)	−718(1)	20(1)
Mo(3)	150(1)	5422(1)	−2179(1)	23(1)
O(1)	−263(3)	4599(5)	−1488(3)	53(1)
O(2)	469(3)	4296(4)	−2792(3)	42(1)
O(3)	1279(3)	6378(4)	−1732(2)	32(1)
O(4)	2225(3)	5429(4)	−297(2)	31(1)
O(5)	3314(3)	6928(4)	−1068(2)	34(1)
O(6)	2719(3)	8006(4)	163(2)	33(1)
O(7)	3326(3)	10156(4)	1076(2)	32(1)
O(8)	2063(3)	8364(4)	1499(2)	33(1)
O(9)	4120(3)	8507(4)	2290(2)	28(1)
N(1)	1716(3)	8900(4)	−1355(3)	25(1)
N(2)	702(3)	7577(4)	−518(3)	23(1)
N(3)	4698(3)	7883(4)	954(3)	23(1)
N(4)	3439(3)	6255(4)	1407(3)	24(1)
C(1)	2281(4)	9517(6)	−1766(3)	32(2)
C(2)	1969(5)	10699(7)	−2143(4)	43(2)
C(3)	1071(5)	11264(6)	−2091(4)	44(2)
C(4)	492(5)	10627(6)	−1668(4)	39(2)
C(5)	819(4)	9434(6)	−1321(3)	28(1)
C(6)	223(4)	8665(6)	−872(4)	28(1)
C(7)	−735(5)	9017(6)	−808(4)	41(2)
C(8)	−1205(5)	8252(7)	−363(4)	47(2)
C(9)	−709(5)	7166(7)	13(4)	43(2)
C(10)	238(4)	6861(6)	−72(4)	31(1)
C(11)	5290(4)	8765(6)	719(3)	27(1)
C(12)	6160(5)	8428(6)	492(4)	37(2)
C(13)	6436(5)	7114(7)	545(4)	42(2)
C(14)	5844(4)	6195(6)	800(4)	36(2)
C(15)	4957(4)	6600(5)	982(3)	24(1)
C(16)	4254(4)	5678(5)	1232(3)	23(1)
C(17)	4386(5)	4335(6)	1276(4)	33(2)
C(18)	3686(5)	3541(6)	1504(4)	40(2)
C(19)	2863(5)	4137(6)	1689(4)	39(2)
C(20)	2765(4)	5489(6)	1632(4)	32(1)

Table 3. Selected Bond Lengths (Å) and Angles (deg) for 1−3

	1 [MoO_3(2,2'-bipy)]		
Mo−O(1)	1.728(4)	O(1)−Mo−O(2)	106.3(2)
Mo−O(2)	1.735(4)	O(1)−Mo−O(3)	102.2(2)
Mo−O(3)	1.822(4)	O(2)−Mo−O(3)	100.5(2)
Mo−N(1)	2.342(4)	O(1)−Mo−N(1)	90.8(2)
Mo−N(2)	2.357(4)	O(2)−Mo−N(1)	161.3(2)
Mo−O(3A)	2.031(3)	O(3)−Mo−N(1)	83.0(2)
O(3)−MoA	2.031(3)	O(1)−Mo−N(2)	158.2(2)
		O(2)−Mo−N(2)	93.3(2)
		O(3)−Mo−N(2)	83.0(2)
		N(1)−Mo−N(2)	68.7(2)
		O(1)−Mo−O(3A)	95.7(2)
		O(2)−Mo−O(3A)	93.3(2)
		O(3)−Mo−O(3A)	153.3(2)
		N(1)−Mo−O(3A)	77.0(2)
		N(2)−Mo−O(3A)	73.4(2)
		N(2)−Mo−O(3A)	73.4(2)
		Mo−O(3)−MoA	148.2(2)
	2 [Mo_2O_6(2,2'-bipy)][a]		
Mo(1)−O(1)	1.699(7)	O(1)−Mo(1)−O(2)	106.6(4)
Mo(1)−O(2)	1.708(7)	O(1)−Mo(1)−O(3)	97.3(2)
Mo(1)−O(3)	1.948(5)	O(2)−Mo(1)−O(3)	97.4(2)
Mo(1)−O(3)#1	1.948(5)	O(1)−Mo(1)−O(3)#1	97.3(2)
Mo(1)−N(1)	2.317(8)	O(2)−Mo(1)−O(3)#1	97.4(2)
Mo(1)−N(2)	2.320(8)	O(3)−Mo(1)−O(3)#1	155.4(3)
Mo(2)−O(4)	1.699(8)	O(1)−Mo(1)−N(1)	91.0(3)
Mo(2)−O(5)	1.707(7)	O(2)−Mo(1)−N(1)	162.4(3)
Mo(2)−O(3)	1.831(5)	O(3)−Mo(1)−N(1)	80.00(15)
Mo(2)−O(3)#2	1.831(5)	O(3)#1−Mo(1)−N(1)	80.80(15)
		O(3)#1−Mo(1)−N(1)	80.00(15)
		O(1)−Mo(1)−N(2)	160.3(3)
		O(2)−Mo(1)−N(2)	93.1(3)
		O(3)−Mo(1)−N(2)	79.8(2)
		O(3)#1−Mo(1)−N(2)	79.8(2)
		N(1)−Mo(1)−N(2)	69.3(3)
		O(4)−Mo(2)−O(5)	104.7(4)
		O(4)−Mo(2)−O(3)	105.1(2)
		O(5)−Mo(2)−O(3)	114.8(2)
		O(4)−Mo(2)−O(3)#2	105.1(2)
		O(5)−Mo(2)−O(3)))#2	114.8(2)
		O(3)−Mo(2)−O(3)#2	111.2(3)
		Mo(2)−O(3)−Mo(1)	157.9(3)
	3 [Mo_3O_9(2,2'-bipy)$_2$][b]		
Mo(1)−O(8)	1.696(4)	O(8)−Mo(1)−O(7)	106.8(2)
Mo(1)−O(7)	1.706(4)	O(8)−Mo(1)−O(6)	100.8(2)
Mo(1)−O(6)	1.901(4)	O(7)−Mo(1)−O(6)	97.7(2)
Mo(1)−O(9)	2.010(4)	O(8)−Mo(1)−O(9)	97.1(2)
Mo(1)−N(4)	2.332(5)	O(7)−Mo(1)−O(9)	94.2(2)
Mo(1)−N(3)	2.337(4)	O(6)−Mo(1)−O(9)	154.6(2)
Mo(2)−O(5)	1.706(4)	O(7)−Mo(1)−N(4)	163.3(2)
Mo(2)−O(6)	1.881(4)	O(6)−Mo(1)−N(4)	82.6(2)
Mo(2)−O(3)	2.027(4)	O(9)−Mo(1)−N(4)	79.7(2)
Mo(2)−N(1)	2.319(4)	O(8)−Mo(1)−N(3)	158.4(2)
Mo(2)−N(2)	2.319(4)	O(7)−Mo(1)−N(3)	94.7(2)
Mo(3)−O(1)	1.697(4)	O(6)−Mo(1)−N(3)	78.1(2)
Mo(3)−O(2)	1.711(4)	O(9)−Mo(1)−N(3)	78.6(2)
Mo(3)−O(3)	1.814(4)	N(4)−Mo(1)−N(3)	69.0(2)
Mo(3)−O(9)#1	1.829(4)	O(5)−Mo(2)−O(4)	106.1(2)
O(9)−Mo(3)#2	1.829(4)	O(5)−Mo(2)−O(6)	100.2(2)
		O(4)−Mo(2)−O(6)	101.0(2)
		O(5)−Mo(2)−O(3)	95.2(2)
		O(4)−Mo(2)−O(3)	93.4(2)
		O(6)−Mo(2)−O(3)	155.0(2)
		O(5)−Mo(2)−N(1)	90.8(2)
		O(4)−Mo(2)−N(1)	160.8(2)
		O(6)−Mo(2)−N(1)	84.7(2)
		O(3)−Mo(2)−N(1)	75.6(2)
		O(5)−Mo(2)−N(2)	160.1(2)
		O(4)−Mo(2)−N(2)	93.3(2)
		O(6)−Mo(2)−N(2)	80.2(2)
		O(3)−Mo(2)−N(2)	78.7(2)
		N(1)−Mo(2)−N(2)	69.4(2)
		O(1)−Mo(3)−O(2)	108.7(2)
		O(1)−Mo(3)−O(3)	110.0(2)
		O(2)−Mo(3)−O(3)	108.3(2)
		O(1)−Mo(3)−O(9)#1	108.5(2)
		O(2)−Mo(3)−O(9)#1	110.5(2)
		O(3)−Mo(3)−O(9)#1	110.8(2)
		Mo(3)−O(3)−Mo(2)	145.6(2)
		Mo(2)−O(6)−Mo(1)	160.0(3)
		Mo(3)#2−O(9)−Mo(1)	135.0(2)

[a] Symmetry transformations used to generate equivalent atoms for **2**: #1 $x, -y + 1/2, z$; #2 $x, -y - 1/2, z$. [b] Symmetry transformations used to generate equivalent atoms for **3**: #1 $x, -1/2, -y + 3/2, z - 1/2$; #2 $x + 1/2, -y + 3/2, z + 1/2$.

collected by filtration and dried at room temperature (yield ca. 10% based on molybdenum).

Preparation of [Mo_3O_9(2,2′-bipy)$_2$] (3). *Method A*: A mixture of MoO_3, 2,2′-bipyridine, $MnCl_2 \cdot 4H_2O$, and H_2O in the mole ratio 1:2:6:2000 (8 mL volume) was placed in a 23 mL Teflon-lined Parr acid digestion bomb and heated for 138 h at 160 °C under autogenous pressure. After cooling to room temperature on the benchtop, colorless octahedra of **3** were collected by vacuum filtration and dried. An unidentified red solid was commonly found within the colorless octahedra of **3**, and therefore a crystal fragment free of this red material by visual observation was used for the X-ray structure determination (yield ca. 20% based on molybdenum).

Method B: See preparation of **1**, method B.

X-ray Structure Determination. X-ray data for **1** were collected on a Rigaku AFC5S four-circle diffractometer. X-ray data for **2** and **3** were collected on a Siemens SMART CCD system. In all cases, graphite monochromated Mo Kα radiation (λ(Mo Kα) = 0.710 73 Å) was used. The crystal parameters and details of the structure solution and refinement of **1**−**3** are summarized in Table 1. An empirical absorption correction using the program DIFABS was applied to all data,[17] and the data were corrected for Lorentz and polarization effects. The structures were solved by direct methods.[18] All non-hydrogen atoms were refined anisotropically. Hydrogen atoms were placed in calculated positions and were refined isotropically. Neutral atom scattering factors were taken from Cromer and Waber,[19] and anomalous dispersion corrections were those of Creagh and McAuley.[20] All calculations were performed using the SHELXTL[21] crystallographic software package.

The structure of **1** was solved and refined in the centric space group *Cc*. This choice was confirmed by the absence of a center of symmetry in the packing diagram of **1** and the absence of significant correlations in the matrix. Furthermore, attempts to refine the structure of **1** in the centric equivalent *C*2/*c* proved unsuccessful. Atomic positional parameters for **1**−**3** are shown in Table 2 and selected bond lengths and angles for **1**, **2** and **3** are shown in Table 3.

Results and Discussion

Hydrothermal synthesis, in common with other soft-chemical techniques, has previously been shown to produce a wide variety of metastable oxide materials.[4,6] Utilization of the hydrothermal method has allowed the isolation of the three organic/inorganic hybrid materials reported herein: [MoO_3(2,2′-bipy)] (**1**), [Mo_2O_6(2,2′-bipy)] (**2**), and [Mo_3O_9(2,2′-bipy)$_2$] (**3**). Hydrothermal syntheses of **1**−**3** were accomplished using Teflon-lined Parr acid digestion bombs as the reaction vessels at temperatures of either 160 or 200 °C and autogenous pressure. Although in our first successful preparation of **1**−**3** (see Experimental Section, methods A) either $FeCl_2 \cdot 4H_2O$ or $MnCl_2 \cdot 4H_2O$ were present in the initial reaction mixture, neither were found in the crystalline products as isolated and characterized by SEM. However, attempts to reproduce the syntheses in the absence of these reaction components have met with mixed success, as evidenced by the alternate preparation methods given for **1** and **3**. It is not uncommon for necessary reactants in hydrothermal processes to be absent from the product, while their specific role in nucleation or

(17) Walker, N.; Stuart, D. *Acta Crystallogr. Sect. A* **1983**, *39*, 158.
(18) "teXsan: Texray Structural Analysis Package"(revised), Molecular Structure Corp., The Woodlands, TX, 1992, or SHELXTL PC, Siemens Analytical X-ray Instruments, Inc., Madison, WI, 1993.
(19) Cromer, D. T.; Waber, J. T. *International Tables for X-ray Crystallography*; Kynoch Press: Birmingham, England, 1974; Vol. IV.
(20) Creagh, D. C.; McAuley, J. W. J. *International Tables for X-ray Crystallography*, Vol. C, Table 4.2.6.8; Kluwer Academic Press: Boston, 1992.
(21) SHELXTL PC, Siemens Analytical X-ray Instruments, Inc., Madison, WI, 1993.

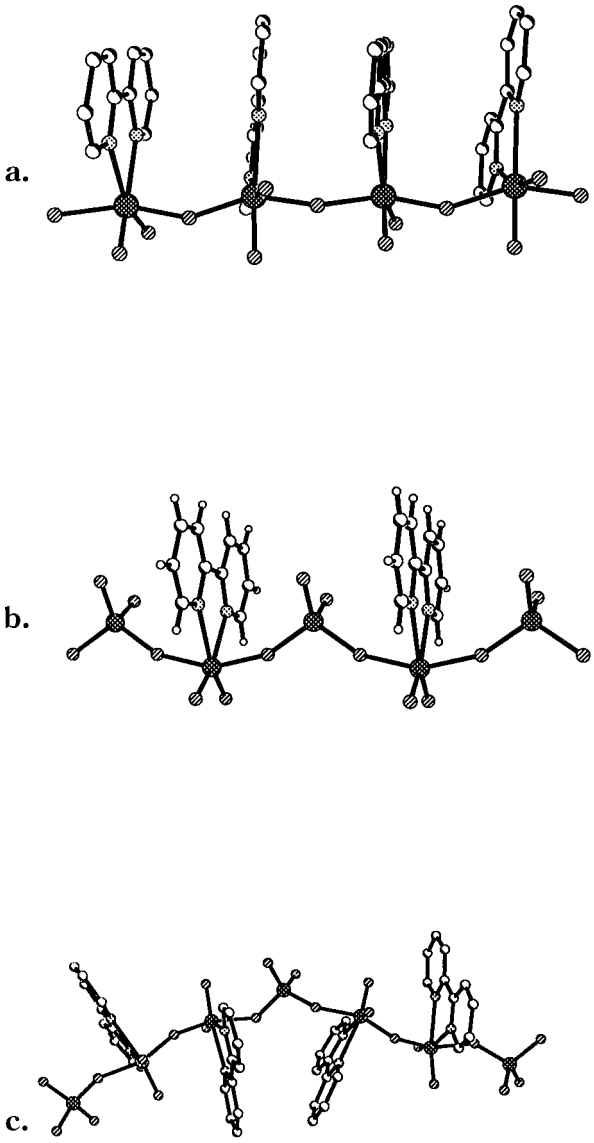

Figure 1. Views of the one-dimensional chains of (a) [MoO_3-(2,2′-bipy)] (**1**) along the *a* axis and (b) [Mo_2O_6(2,2′-bipy)] (**2**) perpendicular to the *b* crystallographic axis, (c) [Mo_3O_9(2,2′-bipy)$_2$] (**3**) along the *a* axis.

providing a repository of metal clusters remains elusive.[22]

Grossly similar conditions were employed in the syntheses of **1**−**3**. Compound **1** [MoO_3(2,2′-bipy)] and **3** [Mo_3O_9(2,2′-bipy)$_2$] were synthesized from MoO_3, 2,2′-bipyridine, and H_2O in the mole ratio 1:0.68:680 at 160 °C for 120 h in a Teflon-lined Parr acid digestion bomb. Compound **2** [Mo_2O_6(2,2′-bipy)] was synthesized from $Na_2MoO_4{\cdot}2H_2O$, MoO_3, 2,2′-bipyridine, $MnCl_2{\cdot}4H_2O$, and H_2O in the mole ratio 1:1:2:1.9:263 at 200 °C for 4 days. While there is no apparent trend between the composition of the product and reaction conditions such as temperature, duration, or stoichiometry, it is clear that the identity of the product obtained in hydrothermal reactions is critically dependent on the specific reaction conditions employed.

As shown in Figure 1a, the structure of [MoO_3(2,2′-bipy)] (**1**) consists of one-dimensional chains of corner-sharing {MoO_4N_2} octahedra. The coordination geometry of each molybdenum is defined by two bridging oxo groups, two terminal oxo groups, and the two pyridyl nitrogen donors of the 2,2′-bipyridine chelate. The molybdenum site exhibits the two short−two intermediate−two long bond length pattern common to the molybdenum oxides. The long Mo−N bond distances can be attributed to the strong trans influence of the terminal oxo groups. The Mo-bridging oxo group distances are unsymmetrical, giving rise to an infinite {···O═Mo···O═Mo} chain, with alternating short−long Mo−O distances of 1.822 and 2.031 Å, respectively.

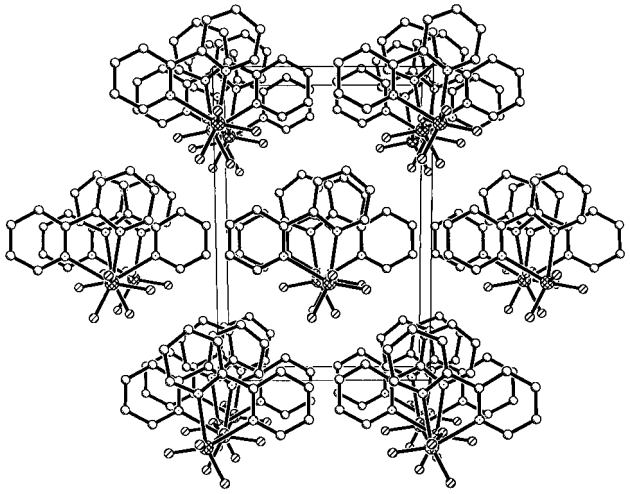

Figure 2. View of the packing of [MoO_3(2,2′-bipy)] (**1**) with the unit cell outlined.

The structure of [Mo_2O_6(2,2′-bipy)] (**2**) is composed of chains of corner-sharing {MoO_4N_2} octahedra and {MoO_4} tetrahedra which alternate to form the one-dimensional chains shown in Figure 1b. As in **1**, the octahedral molybdenum coordination geometry is defined by the two bridging oxo groups, two terminal oxo groups, and the pyridyl nitrogens of the 2,2′-bipyridine chelate. However, in **2** each molybdenum octahedron corner-shares with two adjacent molybdenum tetrahedra whose coordination geometries are defined by two bridging oxo groups and two terminal oxo groups. In contrast to **1**, the bridging oxo groups are symmetrically disposed about each molybdenum site, so that the infinite Mo−O chains appear as alternating two long−two short interactions {···Mo_{Oh}···O═Mo_{Td}═O···} (where Mo_{Oh} represents the octahedral molybdenum site and Mo_{Td} the tetrahedral site).

The structure of [Mo_3O_9(2,2′-bipy)$_2$] (**3**), like that of **2**, is composed of corner-sharing {MoO_4N_2} octahedra and {MoO_4} tetrahedra. However, the polyhedra from which **3** is constructed alternate such that the chain repeat sequence is two {MoO_4N_2} octahedra followed by one {MoO_4} tetrahedron, as shown in Figure 1c. As in **1** and **2**, the octahedral molybdenum coordination geometry can be defined by two bridging oxo groups, two terminal oxo groups, and the pyridyl nitrogens of the 2,2′-bipyridine chelate. The coordination geometry of the tetrahedral molybdenum site in **3**, as in **2**, is defined by two bridging oxo groups and two terminal oxo groups. Bond distances in **3** are consistent with the trends commonly observed for different molybdenum polyhedral types, with short oxo bridges to the tetrahedral molybdenum sites, relative to the oxo-bridging distances to the octahedral sites.

The packing arrangement of **1**, seen in Figure 2, shows the 2,2′-bipyridine rings of **1** fanning out along the chains. The parallel chains align such that each

(22) Soghomonian, V.; Chen, Q.; Haushalter, R. C.; Zubieta, J.; O'Connor, C. J. *Science* **1993**, *259*, 1596.

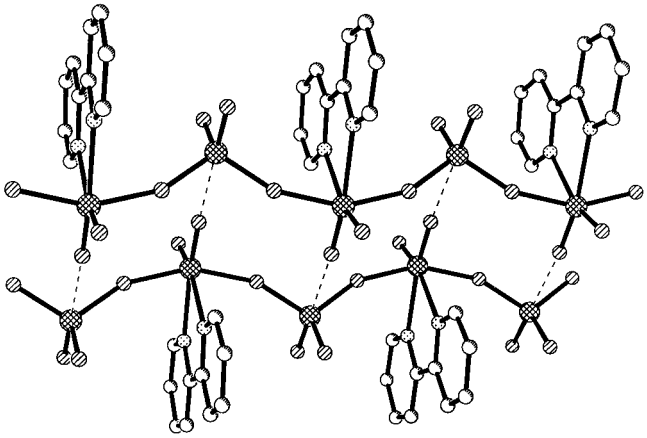

Figure 3. View of two symmetry-related chains in $[Mo_2O_6(2,2'\text{-bipy})]$ (**2**) showing the closest contacts between the tetrahedral molybdenum sites and an oxygen from the $\{MoO_4N_2\}$ octahedra (Mo···O 2.768 Å).

chain has six neighbors, with no close contacts between adjacent chains. In contrast, examination of the packing of **2** reveals significant Mo···O contact distances of 2.768 Å between adjacent symmetry-related chains. The interactions between the molybdenum atom of a $\{MoO_4\}$ tetrahedron and one of the terminal oxygens of an $\{MoO_4N_2\}$ octahedron on a neighboring chain form a virtual dimer of chains as shown in Figure 3. Finally, the chains that comprise compound **3** show pronounced "ruffling" due to the steric constraints imposed by the $\{MoO_4\}$ tetrahedra present in the structure, as shown in Figure 4a. While this change of direction in propagation of the chain is also present in **2** (see Figure 1b), it is more pronounced in **3** due to the increased length of the tether between the $\{MoO_4\}$ sites. Examination of **3** along the crystallographic *c* axis, as illustrated in Figure 4b, reveals virtual channels occupied by π-stacked 2,2′-bipyridine (C−C bonds are drawn as heavy lines for clarity). Removal of the carbon atoms emphasizes the virtual channels shown in Figure 4c.

The one-dimensional structures of **1**−**3** are quite distinct from those of other molybdenum oxide chains, such as $[H_3NCH_2CH_2NH_3][Mo_3O_{10}]$,[7] $K_2[Mo_3O_{10}]$,[14] $(NH_4)_2[Mo_3O_{10}]$,[11] $Na(NH_4)[Mo_3O_{10}]$, and $[H_3N(CH_2)_6NH_3][Mo_4O_{13}]$,[8] all of which exhibit edge-sharing of Mo octahedra as part of the structural motif as shown in Figure 5. Thus the bipyridine ligand serves to "passivate" the molybdenum oxide coordination sphere by blocking further Mo−oxo bond formation.

Figure 5a shows the complex pattern of edge-, corner-, and face-sharing $\{MoO_6\}$ octahedra that produce the one-dimensional polymeric chains comprising the $[Mo_3O_{10}]^{2-}$ structural core of $[H_3NCH_2CH_2NH_3][Mo_3O_{10}]$. Shown in Figure 5b is the infinite chain of edge-sharing $\{MoO_6\}$ octahedra and $\{MoO_5\}$ square pyramids that form the structural core of $K_2[Mo_3O_{10}]$. Both $(NH_4)_2[Mo_3O_{10}]$ and $Na(NH_4)[Mo_3O_{10}]$ share the chain constructed from $[Mo_3O_{10}]^{2-}$ units shown in Figure 5c as their basic structural core. Within the $[Mo_3O_{10}]^{2-}$ motif, there are three $\{MoO_6\}$ octahedra that share two edges, and each of these units is joined to the next $[Mo_3O_{10}]^{2-}$ unit by sharing two edges. The $[Mo_4O_{13}]^{2-}$ units that forms the structural core of $[H_3N(CH_2)_6NH_3][Mo_4O_{13}]$ are composed of four $\{MoO_6\}$ octahedra which edge-share. A symmetry-related $[Mo_4O_{13}]^{2-}$ unit is joined to the first by sharing an edge, forming a unit comprised of eight octahedra. These eight-octahedra units join through shared vertexes to form the infinite chain shown in Figure 5d.

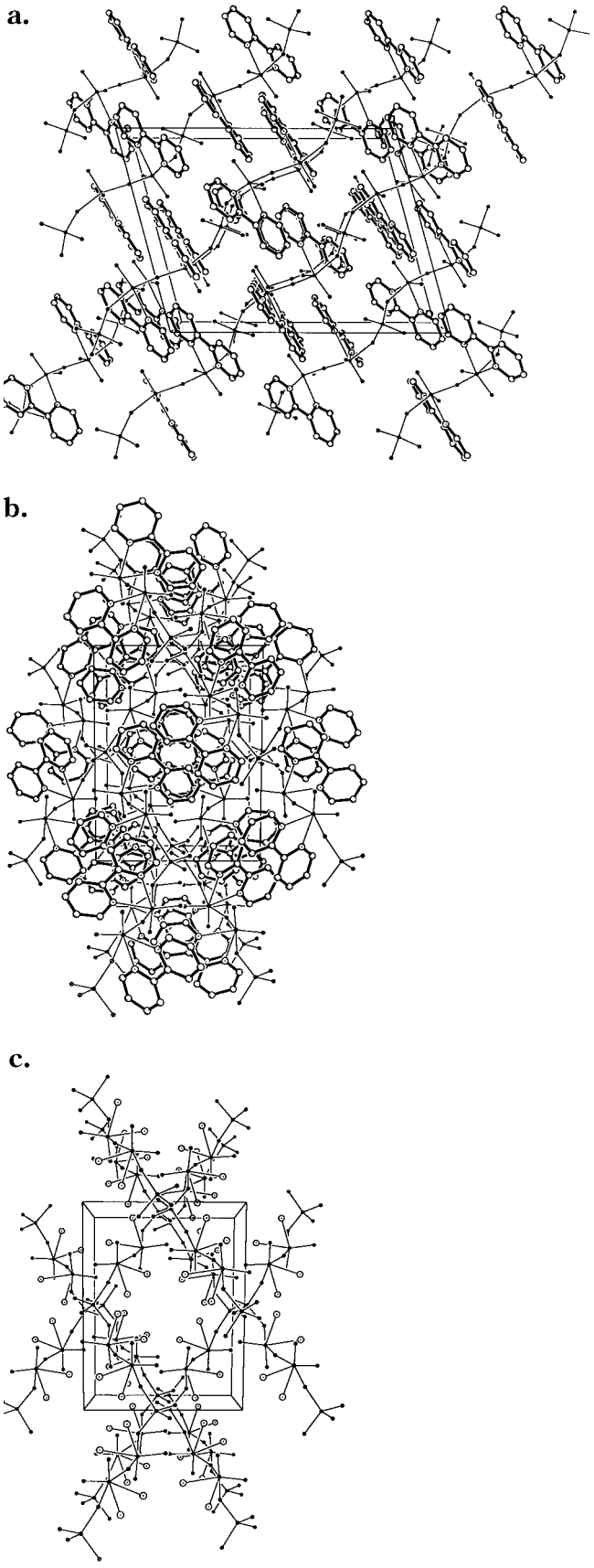

Figure 4. Views of $[Mo_3O_9(2,2'\text{-bipy})_2]$ (**3**) with the unit cell outlined showing the packing (a) along *b* and the "ruffling" of the one-dimensional chains, (b) along *c*, showing the virtual channels occupied by π-stacked 2,2′-bipyridine, (c) along *c*, with the bipyridine carbons removed to emphasize the virtual channels.

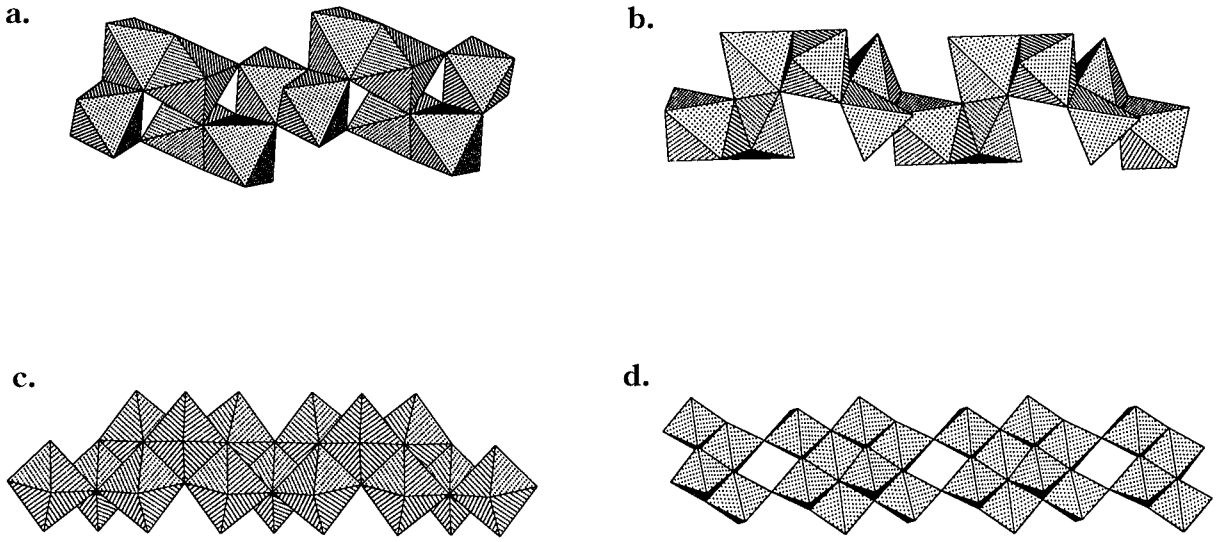

Figure 5. Polyhedral view of the distinct one-dimensional chains adopted by the anions of (a) $[H_3NCH_2CH_2NH_3][Mo_3O_{10}]$, (b) $K_2[Mo_3O_{10}]$, (c) $Na(NH_4)[Mo_3O_{10}]$ and $(NH_4)_2[Mo_3O_{10}]$, and (d) $[H_3N(CH_2)_6NH_3][Mo_4O_{13}]$.

Despite the extensive real and potential applications of solid-phase metal oxides, the rational synthesis of such materials remains elusive. The synthetic challenge reflects the insolubility and lack of reactivity at low temperatures of the starting materials, coupled to the fact that the solid grows simultaneously in three dimensions. Hydrothermal synthesis provides a low-temperature technique for the synthesis of metastable solid phases which retain the structural integrity of the starting materials. By combining this synthetic methodology with the introduction of organic components, new classes of organic/inorganic hybrid materials are accessible. The organic component serves not only to introduce hydrophilic/hydrophobic interactions that necessitate structural reorganization of the oxide phases but also as conventional ligands occupy sites on the metal coordination sphere so as to "passivate" the surface and "direct" aggregation toward lower dimensional structures.

Acknowledgment. This work was supported by NSF Grant CHE9617232.

Supporting Information Available: Complete crystallographic parameters and data for compounds **1**−**3** (21 pages); structure factors for **1**−**3** (21 pages). Ordering information is given on any current masthead page.

CM970260O